

Effective g factor of n -type HgTe/Hg_{1-x}Cd_xTe single quantum wells

X. C. Zhang, K. Ortner, A. Pfeuffer-Jeschke, C. R. Becker,* and G. Landwehr
Physikalisches Institut der Universität Würzburg, Am Hubland, 97074 Würzburg, Germany

(Received 23 July 2003; revised manuscript received 24 October 2003; published 30 March 2004)

The effective g factor of modulation doped n -type HgTe single quantum wells, SQW's, has been determined by the coincidence method in tilted magnetic fields to lie between 15 and 35. For symmetrically doped samples the effective g factor has been found to be constant for different filling factors; however, for asymmetric SQW's, a large increase with increasing filling factor has been observed. This can be ascribed to a combination of Zeeman spin splitting and Rashba spin-orbit splitting. Reasonable agreement has been achieved between theoretical calculations based on the $8 \times 8 \mathbf{k} \cdot \mathbf{p}$ method and experimental results.

DOI: 10.1103/PhysRevB.69.115340

PACS number(s): 73.61.Ga, 73.21.Fg, 71.70.Ej, 71.18.+y

I. INTRODUCTION

HgTe based type III heterostructures have aroused much interest due to their unique band structure.¹ Initially, most magnetotransport studies on these type III heterostructures have concentrated on either unintentionally or modulation doped HgTe/CdTe superlattices which have always shown mixed conduction behavior due to more than two carrier species²⁻⁴ resulting in net electron concentrations up to $3 \times 10^{17} \text{ cm}^{-3}$ and a maximum mobility of about $1.1 \times 10^4 \text{ cm}^2/\text{Vs}$. The quantum Hall effect, QHE, has been observed in HgTe/Hg_{1-x}Cd_xTe superlattices,^{5,6} but the Hall plateaus were not well developed and ρ_{xx} did not go to zero in the QHE regime due to either parallel conduction or inhomogeneous carrier distribution along the growth direction.

Recently the availability of a high mobility two-dimensional (2D) electron gas, 2DEG, in HgTe SQW's (Ref. 7) has made it possible to systematically study Zeeman spin splitting as well as other aspects of their transport behavior. As a result of their small effective mass, these samples show pronounced Shubnikov-de Haas, SdH, oscillations whose onset occurs near 1 T. Spin splitting has been resolved at about 2–3 T, and the corresponding filling factors ν can be unambiguously assigned to well developed quantum Hall plateaus. Pfeuffer-Jeschke *et al.*⁸ have reported values of the effective mass m^* and its dependence on charge-carrier concentration for a series of quantum wells (QW's) with a well width of 9 nm. m^* increases from $0.016 m_0$ at $1 \times 10^{11} \text{ cm}^{-2}$ to $0.035 m_0$ at $1 \times 10^{12} \text{ cm}^{-2}$. Very pronounced Rashba spin-orbit, SO, splitting⁹ has recently been reported in the conduction subband of n -type modulation doped HgTe quantum wells with an inverted band structure.^{10,11} Due to their inverted band structure, the heavy-hole character of the first conduction subband leads to a very large Rashba SO splitting. By means of a gate voltage the asymmetry of the QW was varied and the resulting Rashba splitting was deduced from the Fourier transformation of SdH oscillations. The data has been quantitatively explained by means of self-consistent Hartree calculations based on an $8 \times 8 \mathbf{k} \cdot \mathbf{p}$ model.^{11,12} Moreover, the observed Rashba SO splitting was larger than Zeeman spin splitting even at moderately high magnetic fields.

Zeeman spin splitting in a 2DEG was first observed in measurements of SdH oscillations in Si field effect transis-

tors based on a metal-oxide-semiconductor structure.¹³ Zeeman spin splitting is expressed as $g^* \mu_B B$, where g^* is the effective g factor, μ_B the Bohr magneton, and B the external magnetic field. Most of the previous experimental work has been devoted to study of the exchange enhancement of g^* due to different occupancies of two spin states of a Landau level, which was predicted by Ando and Uemura,¹⁴ and has been observed in different two-dimensional systems, such as silicon inversion layers,¹⁵ as well as GaAs/AlGaAs (Refs. 16,17) and GaInAs based heterostructures.¹⁸ Recently the effective g factor has received considerable attention; calculations have predicted different values for the transverse and longitudinal components of g^* in a QW due to size quantization effects¹⁹ and intensive experimental activities have been devoted to the study of the anisotropy of the g factor.^{20,21}

In contrast to numerous investigations on III-V systems, measurements of the effective g factor in HgTe based QW's have, to our knowledge, not been reported. In this investigation g^* has been deduced from measurements of the SdH effect in a tilted magnetic field, i.e., the coincidence method, which is based on the fact that Landau level, LL, splitting is proportional to the component of the magnetic field perpendicular to the 2DEG plane, whereas spin splitting depends on the total magnetic field. In this article we demonstrate that g^* is large and constant for quantum wells with a symmetric potential; however, it is enhanced for asymmetric quantum wells. This difference in magnetic-field dependence of the g factor can be ascribed to a combination of the Rashba effect and Zeeman spin splitting, as has been confirmed by band-structure calculations based on the $8 \times 8 \mathbf{k} \cdot \mathbf{p}$ method.

II. EXPERIMENTAL AND THEORETICAL DETAILS

HgTe single quantum wells (SQW's) were grown by molecular-beam epitaxy, MBE, on Cd_{0.96}Zn_{0.04}Te(001) substrates after an approximately 60 nm thick CdTe buffer was deposited. All samples were modulation doped in one or both of the Hg_{0.32}Cd_{0.7}Te barriers with iodine as has been described elsewhere.⁷ This doped layer is separated from the HgTe layer by an 8 nm thick Hg_{0.3}Cd_{0.7}Te spacer. Finally a 20 nm thick CdTe cap layer was grown. The total thickness of these heterostructures is less than 120 nm and consequently they are fully strained. The HgTe width was deter-

TABLE I. Sample parameters.

Sample	d_w nm	Doping mode	n_s 10^{11} cm^{-2}	μ $10^4 \text{ cm}^2/\text{Vs}$	m^* m_0
Q1651	11	Asymmetric	3.45	8.14	0.026
Q1283	9	Symmetric	6.59	7.35	0.030
Q1424	4.5	Asymmetric	18.5	2.82	0.048

mined by simulations of the (002) and (004) Bragg reflections.^{11,22}

Two SQW's with similar well widths d_w and an inverted band structure, i.e., $d_w > 6$ nm, were grown and analyzed as described below. The band structure of these two QW's are nearly equivalent because the band structure in the inverted regime depends only weakly on the well width. One of these SQW's was symmetrically modulation doped whereas the other was asymmetrically modulation doped. The barriers were modulation doped with an equal amount of iodine which resulted in a 2DEG concentration which was twice as large in the symmetric QW.

The difference in magnetic-field dependence of the g factors in symmetric and asymmetric QW's is attributed in a following section to the Rashba SO splitting present in the asymmetric QW's. For comparison purposes an asymmetrically modulation doped SQW with a normal band structure, $d_w < 6$ nm, was also characterized. Since the Rashba effect¹¹ is much smaller in QW's with a normal band structure a larger 2DEG concentration was chosen.

The magnitude of the energy gap, E_{H1-E1} , is 55 ± 10 meV for all samples whereas E_{H1-E1} is negative for an inverted band structure. H and E refer to heavy hole and electron subbands, respectively. In all samples, only the first conduction subband was occupied and the second conduction subband was at least 100 meV above the Fermi energy. The sample parameters are summarized in Table I.

After growth, samples with Hall geometry were patterned by wet chemical etching and Ohmic contacts were made by indium thermal bonding. Magnetotransport measurements were performed with standard ac lock-in techniques in magnetic fields up to 14 T at a temperature of 1.6 K. The sample current was kept sufficiently low in order to avoid electrical heating. For measurement in a tilted magnetic field, the samples were mounted on a revolving holder and rotated about their long axis, always in the same direction in order to minimize any mechanical errors in the goniometer.

Spin splitting energies were calculated in the framework of an $8 \times 8 \mathbf{k} \cdot \mathbf{p}$ model with the incorporation of a perpendicular magnetic field. A detailed description of the theory and the band-structure parameters employed in the calculations can be found elsewhere.^{11,12,23}

III. RESULTS AND DISCUSSION

A. SdH oscillations and QHE

Typical experimental plots of SdH oscillations and the QHE are shown in Figs. 1 and 2 for the asymmetric Q1651 and symmetric Q1283, respectively. The spin splitting re-

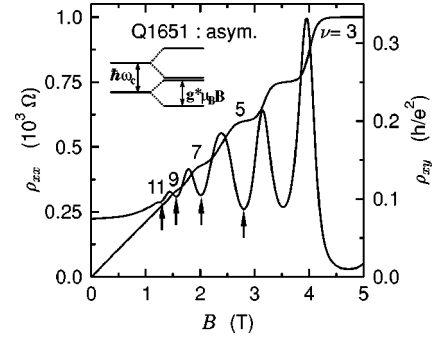


FIG. 1. SdH oscillations and the QHE for the asymmetric sample Q1651. The arrows at the minima of SdH oscillations show the positions that correspond to the indicated odd filling factors. The inset illustrates the fact that the Zeeman spin splitting $g^* \mu_B B$ is larger than half of the LL splitting, $\hbar \omega_c$.

solved in Fig. 2 for $B \geq 2$ T is obscured in Fig. 1 due to coincidental degeneracy of the Zeeman and Landau split levels. The spin splitting behavior of these two QW's is quite different. In Fig. 1, the minima in ρ_{xx} at low magnetic fields always correspond to odd filling factors in the asymmetric QW, as indicated by arrows. In contrast the minima for the symmetric sample Q1283 always correspond to even filling factors. This indicates that Zeeman spin splitting is larger than half of the Landau-level splitting, the cyclotron energy $\hbar \omega_c$, in the asymmetric sample, but smaller for the symmetric one. This is schematically shown in the insets in Figs. 1 and 2. This behavior is reproducible for the series of samples investigated. Furthermore the measurements in a tilted magnetic field, which will be presented below, confirm the above conclusion.

By means of self-consistent Hartree calculations¹¹ the Rashba spin-orbit splitting has been calculated to be 3.8 and 8.2 meV for the asymmetric QW's Q1651 and Q1424, respectively, and 0.0 meV for the symmetric QW Q1283. An experimental value of 8 meV has been determined for Q1424 from the occupancies of the spin split conduction subband via fast Fourier transformation of the SdH oscillations. The effective mass m^* has been deduced from the temperature

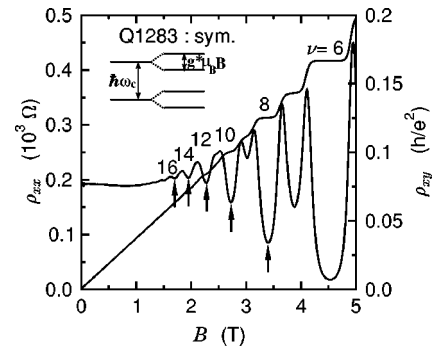


FIG. 2. SdH oscillations and the QHE for the symmetric sample Q1283. The arrows at the minima of SdH oscillations show the positions that correspond to the indicated even filling factors. The inset illustrates the fact that the Zeeman spin splitting $g^* \mu_B B$ is smaller than half of the LL splitting, $\hbar \omega_c$.

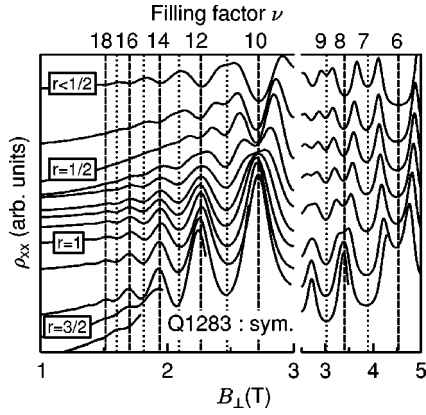


FIG. 5. $\rho_{xx}(B_{\perp})$ traces for various tilt angles for sample Q1283 where different coincidence conditions, r , are fulfilled. From top to bottom the curves correspond to the tilt angles of 4.7° , 39.7° , 44.7° , 49.7° , 54.7° , 59.7° , 64.7° , 69.7° , 72.7° , 74.7° , 76.7° , 78.7° , 79.7° , and 80.7° .

magnetic field, B_{\parallel} . But when the magnetic length $l = (\hbar/eB_{\parallel})^{1/2}$ is comparable to or less than the well width d_w , magnetic quantum confinement may result, and the SdH oscillations may become irregular. Thus, for example, this method requires B_{\parallel} to be less than about 8.1 T when the well width is 9 nm. This means that θ must be less than 35.6° if the total magnetic field is 10 T. This requirement can not be fulfilled for a 9 nm thick quantum well such as Q1283. Consequentially another method is employed in this investigation which is less sensitive to irregularities in the period of the SdH oscillations, as described below. The same arguments concerning the influence of the in-plane magnetic field can be applied to the coincidence method. This will also be discussed later.

In order to determine a precise value of the coincidence position, the absolute magnitudes of the resistivity extrema shown, for example, in Figs. 4 and 5 have been plotted as a function of $1/\cos(\theta)$ near $r=1$. Typical results are shown for Q1651 and Q1283 in Figs. 6 and 7, respectively, for the minima and maxima of ρ_{xx} for different integer filling factors. These curves have also been shifted vertically and multiplied by a scaling factor for ease of comparison. The magnitude of the resistivity extrema which are plotted as a function of $1/\cos(\theta)$ pass through an obvious maximum or minimum.

The coincidence position obviously depends on the filling factor for sample Q1651 but not for Q1283; this is evident from the position of the arrows in Figs. 6 and 7 which occur at progressively smaller angles as the filling factor increases for Q1651, but remains constant within experimental uncertainty for sample Q1283. In order to determine g^* it is necessary to know the effective mass. We have employed the value of m^* deduced from the temperature dependence of SdH oscillations,¹⁵ see Table I. The resulting g^* factors are shown in Fig. 8. g^* lies in the range of 15–35. These values are relatively large compared to other 2D systems as expected for narrow gap systems. It is obvious that g^* increases with filling factor for the asymmetric samples Q1651

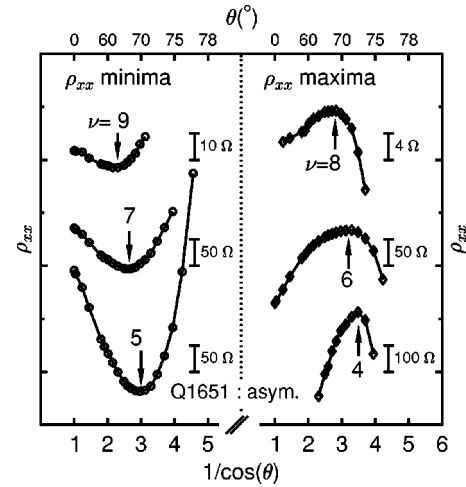


FIG. 6. Values of the minima (left side) and maxima in ρ_{xx} (right side) for several filling factors for sample Q1651 as a function of $1/\cos(\theta)$ near $r=1$, where θ is the tilt angle. The arrows indicate the values used to calculate g^* . With increasing filling factor the extrema occur at lower values of $1/\cos(\theta)$, which suggest that g^* increases with increasing filling factor.

and Q1424, but remains essentially constant versus filling factor for the symmetric sample Q1283.

Many-body effects are known to result in an oscillatory behavior in g^* for electrons with filling factor ν , which is related to the different occupancy of the two spin states of one Landau level.¹⁴ These effects should be larger for smaller filling factors, however, in this investigation g^* was determined for relatively large filling factors, i.e., $20 \geq \nu \geq 4$. Furthermore g^* is so large that exchange effects are expected to be unimportant.

The nonparabolicity of the band structure can not explain the difference in magnetic-field dependence behavior of g^*

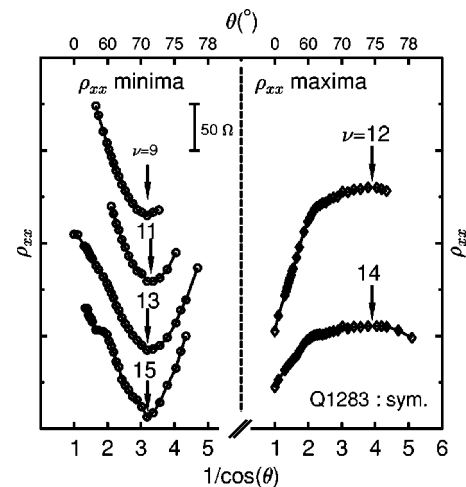


FIG. 7. Values of the minima (left side) and maxima in ρ_{xx} (right side) for several filling factors for sample Q1283 as a function of $1/\cos(\theta)$ near $r=1$, where θ is the tilt angle. The arrows indicate the values used to calculate g^* . The $1/\cos(\theta)$ values of the extrema are nearly constant, which suggests that g^* is independent of the filling factor.

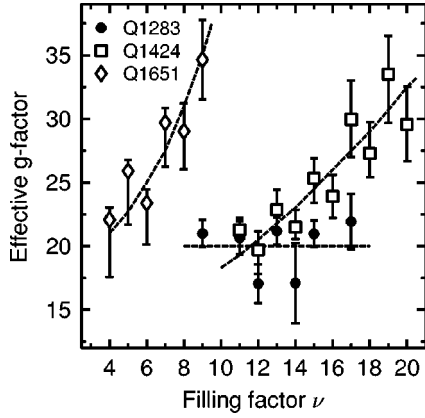


FIG. 8. The effective g factor vs filling factor of the symmetric sample Q1283 and the asymmetric specimens Q1424 and Q1651. The symbols are experimental values determined by the coincidence method. The dashed curves are merely guides to the eye.

shown in Fig. 8. The theory of Kacman and Zawadzki²⁶ relates the effective g factor to the effective mass through the following relationship:

$$g^* = 2 \left[1 + \left(1 - \frac{m_0}{m^*(k)} \right) \frac{\Delta}{3\varepsilon'(k) + 2\Delta} \right], \quad (2)$$

where $\varepsilon'(k) = \varepsilon(k) - \hbar^2 k^2 / 2m_0$, $\varepsilon(k)$ is measured from the conduction-band edge and Δ is the spin-orbit splitting energy. For this narrow gap system, Eq. (2) can be reduced to

$$g^* \approx 3 - \frac{m_0}{m^*} \approx -\frac{m_0}{m^*}, \quad (3)$$

since $\Delta \gg E_g$ and $m_0/m^* \gg 1$. m^* increases with increasing magnetic field, in particular with increasing in-plane component, B_{\parallel} .²⁷ Consequently g^* decreases in value with increasing magnetic field and vice versa with filling factor. Magneto-optical measurements in a perpendicular magnetic field on a similar sample with a well width of 9 nm and carrier density of $6.45 \times 10^{11} \text{ cm}^{-2}$ demonstrated that m^* increases only a small amount from $0.026 m_0$ at 0 T to $0.029 m_0$ at 5 T.²⁸ Even if the influence of B_{\parallel} on m^* is larger, it can not account for the different experimental behavior in asymmetric and symmetric samples, i.e., the large and sharp increase in g^* with filling factor as opposed to the constant value, respectively, shown in Fig. 8. Rashba SO splitting in asymmetric QW's may depend on the in-plane magnetic field. An increase in the Rashba effect with increasing B_{\parallel} could explain the observed behavior of g^* with filling factor.

The influence of band nonparabolicity on the value of g^* determined from SdH oscillations is assumed to be constant, i.e., independent of B , as has been argued in Appendix B of Ref. 29. Smith *et al.*³⁰ have measured the g factor of electrons in an InAs/GaSb SQW by means of a tilted magnetic-field experiment and found g^* to be constant within experimental error, i.e., 8.2 ± 0.5 , when B was increased from 5 to 10 T. This is also true for our symmetric sample Q1283. The g factor of this sample is almost constant between magnetic

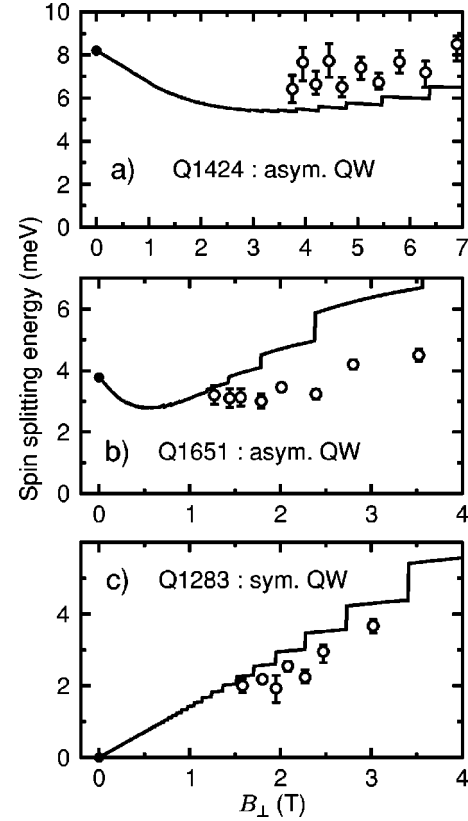


FIG. 9. Experimental values of the spin splitting energy at E_F vs magnetic field for samples Q1424, Q1651, and Q1283 (empty circles), and theoretical values of zero-field spin splitting energies (filled circles). Theoretical calculations vs magnetic field (solid lines) are also shown for comparison.

fields of 1 and 3 T. Only two data points are slightly lower than the other five points. However these two points correspond to the broader peaks in the right panel of Fig. 7 and consequently have a larger experimental uncertainty as indicated in Fig. 8. As can be seen, g^* for sample Q1283 is constant within experimental error over the investigated magnetic-field range.

C. Spin splitting behavior in a magnetic field

The spin splitting energy $\Delta E = g^* \mu_B B$ has been plotted as a function of the normal component of the magnetic field for a symmetric and two asymmetric samples in Fig. 9. The calculated zero-field spin splitting energy at the Fermi level is also indicated in Fig. 9. An extrapolation of the data to $B=0$ for the symmetric Q1283 indicates the absence of Rashba splitting; however, for the asymmetric samples there is a finite intercept at zero magnetic field. Because of this finite experimental zero-field spin splitting in the asymmetric samples it is obvious that the behavior of the magnetic-field dependence of the spin splitting cannot be explained by the Zeeman spin splitting alone. It is essential to take both Rashba and Zeeman spin splitting into account.

Theoretical calculations based on the $8 \times 8 \mathbf{k} \cdot \mathbf{p}$ method in a perpendicular magnetic field have been performed and are compared with the experimental data in Fig. 9. A detailed

description of the theoretical model and band-structure parameters employed in the calculation can be found elsewhere.^{11,12} The solid lines in Fig. 9 have been calculated for zero temperature. This introduces steps in the curves whenever the Fermi level jumps to a higher Landau level with increasing magnetic field. At low magnetic fields the calculated spin splitting energy for the asymmetric QW's decreases with increasing B and at an intermediate field this energy reaches a minimum before increasing at higher fields. This behavior is very similar to that calculated for asymmetric InGaAs/InAlAs QW's by Pfeffer and Zawadzki.³¹ The basic tendency of ΔE versus B_{\perp} is qualitatively described by the theoretical calculations, although the agreement is not as good as one would like, particularly at high magnetic fields for the asymmetric QW's. This could be due to the neglect of the effect of B_{\parallel} in the analysis employed in the coincidence method.

Recently, spin-resonance experiments on symmetric and asymmetric InSb quantum wells have been reported by Khodaparast *et al.*³² Photoconductivity was measured as a function of magnetic field when the samples were illuminated with monochromatic infrared radiation. In order to observe spin resonance, the Fermi energy had to be located between the spin-up and spin-down levels of a particular Landau state. In order to achieve this, the samples were tilted. As in our experiments, it was demonstrated that the g factor was independent of B for samples with a symmetric potential; however, in asymmetric specimens the spin splitting energy was substantially enhanced at lower magnetic fields. The asymmetry induced shifts of the spin splitting increased linearly with the Landau index, as expected for a semiconductor with a regular band sequence. Their results for the spin splitting in symmetric QW's agreed well with the results of a $\mathbf{k}\cdot\mathbf{p}$ calculation based on the Pidgeon-Brown model.³³ It is significant that their results were obtained by a method not based on the beating of Shubnikov de-Haas oscillations.

It should be noted that in our calculations, the influence of the parallel magnetic field has not been taken into account. It can be seen from the data in Fig. 6 for the asymmetric sample Q1651 at small filling factors, that the coincidence position occurs at a larger θ . This means that the parallel magnetic field $B_{\parallel}=B_{\perp}\tan\theta$ is larger for small filling

factors. Therefore B_{\parallel} would have a larger influence on spin splitting measurements by the coincidence method at higher fields. First of all, B_{\parallel} could influence Rashba SO splitting. Pfeffer and Zawadzki³¹ have calculated spin splitting in a parallel magnetic field for InGaAs/InAlAs QW's and found that it increases with B_{\parallel} .

Even though this system is quite different from HgTe based QW's, their calculated relative dependence on B_{\parallel} is similar to the experimental values for the asymmetric sample shown in Fig. 9. Second, a distortion of the Fermi-surface contour under the influence of B_{\parallel} will manifest itself through an increase in the electron effective mass. Smrčka *et al.*³⁴ have demonstrated that this increase in the effective mass is only 5% for an in-plane component of B up to 5 T for a GaAs/AlGaAs heterojunction. The influence of the in-plane component of the magnetic field on Rashba SO splitting and the effective mass in HgTe QW's is unknown. In order to quantitatively describe the experimental data, calculations which include B_{\parallel} are required.

IV. CONCLUSIONS

In conclusion, the effective g factor for three different n -type modulation doped HgTe SQW's have been determined by the coincidence method in a tilted magnetic field to be between 15 and 35. The experimentally determined dependence of g^* on magnetic field is quite different for symmetrically and asymmetrically doped samples. In the former case, $g^*=|20|\pm 5$ independent of LL filling factor, but in the latter case, a large dependence on ν is observed. This has been ascribed to a combination of Zeeman spin splitting and Rashba SO splitting. The data can be qualitatively explained by means of calculations involving the $8\times 8\mathbf{k}\cdot\mathbf{p}$ method and the perpendicular component of the magnetic field.

ACKNOWLEDGMENTS

We are grateful to G. Remenyi for his expert assistance with measurements in the Grenoble High Magnetic Field Laboratory, HMFL. One of the authors, X. C. Zhang, was supported by the Volkswagen Foundation, and the support of the Deutsche Forschungsgemeinschaft, Grant No. SFB 410, is also gratefully acknowledged.

*Electronic address: becker@physik.uni-wuerzburg.de

¹N.F. Johnson, P.M. Hui, and H. Ehrenreich, Phys. Rev. Lett. **61**, 1993 (1988).

²C.A. Hoffman, J.R. Meyer, F.J. Bartoli, J.W. Han, J.W. Cook, J.F. Schetzina, and J.N. Schulman, Phys. Rev. B **39**, 5208 (1989).

³C.A. Hoffman, J.R. Meyer, F.J. Bartoli, Y. Lansari, J.W. Cook, and J.F. Schetzina, Phys. Rev. B **44**, 8376 (1991).

⁴C.A. Hoffman, J.R. Meyer, and F.J. Bartoli, Appl. Phys. Lett. **60**, 2282 (1992).

⁵N.P. Ong, John K. Moyle, J. Bajaj, and J.T. Cheung, J. Vac. Sci. Technol. A **5**, 3079 (1987).

⁶K.C. Woo, S. Rafol, and J.P. Faurie, J. Vac. Sci. Technol. A **5**, 3093 (1987).

⁷F. Goschenhofer, J. Gerschütz, A. Pfeuffer-Jeschke, R. Helmig,

C.R. Becker, and G. Landwehr, J. Electron. Mater. **27**, 532 (1998).

⁸A. Pfeuffer-Jeschke, F. Goschenhofer, S.J. Cheng, V. Latussek, J. Gerschütz, C.R. Becker, R.R. Gerhardtts, and G. Landwehr, Physica B **256-258**, 486 (1998).

⁹E.I. Rashba, Fiz. Tverd. Tela **2**, 1224 (1960) [Sov. Phys. Solid State **2**, 1109 (1960)]; Yu.A. Bychkov and E.I. Rashba, Pis'ma Zh. Eksp. Teor. Fiz. **39**, 66 (1984) [JETP Lett. **39**, 78 (1984)].

¹⁰M. Schultz, F. Heinrichs, U. Merkt, T. Colin, T. Skauli, and S. Lövdold, Semicond. Sci. Technol. **11**, 1168 (1996).

¹¹X.C. Zhang, A. Pfeuffer-Jeschke, K. Ortner, V. Hock, H. Buhmann, C.R. Becker, and G. Landwehr, Phys. Rev. B **63**, 245305 (2001).

¹²A. Pfeuffer-Jeschke, Doctoral dissertation, Physikalisches Institut

- der Universität Würzburg, 2000.
- ¹³F.F. Fang and P.J. Stiles, *Phys. Rev.* **174**, 823 (1968).
- ¹⁴T. Ando and Y. Uemura, *J. Phys. Soc. Jpn.* **37**, 1044 (1974).
- ¹⁵T. Ando, A.B. Fowler, and F. Stern, *Rev. Mod. Phys.* **54**, 437 (1982).
- ¹⁶R.J. Nicholas, R.J. Haug, K.V. Klitzing, and G. Weimann, *Phys. Rev. B* **37**, 1294 (1988).
- ¹⁷D.R. Leadley, R.J. Nicholas, J.J. Harris, and C.T. Foxon, *Phys. Rev. B* **58**, 13 036 (1998).
- ¹⁸R.J. Nicholas, M.A. Brummell, J.C. Portal, K.Y. Cheng, A.Y. Cho, and T.P. Pearsall, *Solid State Commun.* **45**, 911 (1983).
- ¹⁹E.L. Ivchenko and A.A. Kiselev, *Sov. Phys. Semicond.* **26**, 827 (1992).
- ²⁰V.F. Sapega, T. Ruf, M. Cardona, K. Ploog, E.L. Ivchenko, and D.N. Mirlin, *Phys. Rev. B* **50**, 2510 (1994).
- ²¹P.Le. Jeune, *Semicond. Sci. Technol.* **12**, 380 (1997).
- ²²C.R. Becker, V. Latussek, A. Pfeuffer-Jeschke, G. Landwehr, and L.W. Molenkamp, *Phys. Rev. B* **62**, 10 353 (2000).
- ²³X.C. Zhang, A. Pfeuffer-Jeschke, K. Ortner, C.R. Becker, and G. Landwehr, *Phys. Rev. B* **65**, 045324 (2002).
- ²⁴S. Brosig, K. Ensslin, A.G. Jansen, C. Nguyen, B. Brar, M. Thomas, and H. Kroemer, *Phys. Rev. B* **61**, 13 045 (2000).
- ²⁵M. Schultz, U. Merkt, A. Sonntag, U. Rössler, R. Winkler, T. Colin, P. Helgesen, T. Skauli, and S. Løvold, *Phys. Rev. B* **57**, 14 772 (1998).
- ²⁶P. Kacman and W. Zawadzki, *Phys. Status Solidi B* **47**, 629 (1971).
- ²⁷G. Salis, B. Ruhstaller, K. Ensslin, K. Campman, K. Maranowski, and A.C. Gossard, *Phys. Rev. B* **58**, 1436 (1998).
- ²⁸M. von Truchsess, Ph.D. thesis, Physikalisches Institut der Universität Würzburg, 1999.
- ²⁹B. Das, S. Datta, and R. Reifenberger, *Phys. Rev. B* **41**, 8278 (1990).
- ³⁰T.P. Smith III, and F.F. Fang, *Phys. Rev. B* **35**, 7729 (1987).
- ³¹P. Pfeuffer and W. Zawadzki, *Phys. Rev. B* **59**, R5312 (1999).
- ³²G.A. Khodaparast, R.E. Doezema, S.J. Chung, K.J. Goldhammer, and M.B. Santos, in *Proceedings of 10th International Conference on Narrow Gap Semiconductors and Related Small Energy Phenomena, IPAP Conference Series 2*, edited by N. Miura, S. Yamada, and S. Takeyama (The Institute of Pure and Applied Physics, Tokyo, Japan, 2001), Vol. IPAP-CS2.
- ³³C.R. Pidgeon and R.N. Brown, *Phys. Rev.* **146**, 575 (1966).
- ³⁴L. Smrčka, P. Vašek, J. Koláček, T. Jungwirth, and M. Cukr, *Phys. Rev. B* **51**, 18 011 (1995).